SHOCK, Vol. 42, No. 1, pp. 65–74, 2014

EXPRESSION OF HEMOPEXIN IN ACUTE REJECTION OF RAT LIVER ALLOGRAFT IDENTIFIED BY SERUM PROTEOMIC ANALYSIS

Min Xu,*† Changjun Tan,* Jinwu Hu,* Salamah Mohammad Alwahsh,‡ Jun Yan,§ Jie Hu,* Zhi Dai,* Zheng Wang,* Jian Zhou,*‖ Jia Fan,*‖ and Xiaowu Huang*

**Liver Cancer Institute, Zhongshan Hospital, Fudan University, Shanghai, China; †Departments of General and Visceral Surgery, and ‡Gastroenterology and Endocrinology, University Medical Center Goettingen, Goettingen, Germany; and §Department of Surgery, Fujian Provincial Tumor Hospital, Teaching Hospital of Fujian Medical University, Fuzhou; and ‖Shanghai Key Laboratory of Organ Transplantation, Zhongshan Hospital, Fudan University, Shanghai, China*

Received 6 Jan 2014; first review completed 24 Jan 2014; accepted in final form 6 Mar 2014

ABSTRACT—Acute rejection (AR) and acceptance of allograft after liver transplantation (LTx) remain critical issues that need addressing to improve prognosis. We therefore performed rat orthotopic LTx and proteomic analyses to screen for immune response–related biomarkers in sera. Markers identified were validated at the mRNA and/or protein levels, and the molecules of interest were functionally explored. Compared with syngeneic controls, signs of AR as well as spontaneous acceptance were observed in hematoxylin and eosin–stained sections of liver allografts. In accordance with the severity of AR, 30 protein spots displaying significant changes in abundance were identified using two-dimensional differential gel electrophoresis. Ultimately, 14 serum proteins were sequenced and five spots of interest were identified as hemopexin (HPX). Expression of HPX was significantly and inversely associated with the severity of AR at both the mRNA and protein levels. *In vitro*, *Mt-1*, *Ho-1*, *Fth*, *Ifn-γ*, and *Il-17* transcripts were significantly upregulated in lysates of lymphocytes stimulated with HPX, whereas *Il-10* markedly was remarkably downregulated. Interferon-γ, IL-10, and IL-17 proteins in the supernatant of HPX-stimulated lymphocytes were significantly altered in keeping with the mRNA level. Our data facilitated the generation of a proteomic profile to enhance the understanding of rat liver AR. In view of finding that the HPX serum level is negatively associated with the severity of AR of rat liver allograft, we propose that *in vitro* treatment with HPX regulates cytokine expression in rat lymphocytes.

KEYWORDS—Rat liver allograft, acute rejection, serum 2D-DIGE, HPX, lymphocytes

ABBREVIATIONS—2D-DIGE—two-dimensional differential gel electrophoresis; α1-M—alpha-1-macroglobin; ACI—August Copenhagen Irish; AR—acute rejection; BN—Brown Norway; ELISA—enzyme-linked immunosorbent assay; HE—hematoxylin and eosin; HO-1—heme oxygenase-1; HPX—hemopexin; IFN-γ—interferon-γ; KNG 2—Kininogen 2; LTx—liver transplantation; MALDI—matrix-assisted laser desorption/ionization; MBP-A—mannose-binding protein; MLR—mixed lymphocyte reaction; MS—mass spectrometry; MT-1—metallothionein-1; PHp—preprohaptoglobin

INTRODUCTION

Liver transplantation (LTx) is an effective therapeutic option for end-stage liver disease. Although immunosuppressive therapies have substantially improved outcomes in recent years, acute rejection (AR) remains a common complication of LTx, reported in approximately 30% of recipients (1, 2). Acute rejection predominantly occurs during the early posttransplant period (usually within 6 weeks) (3). Diagnosis of AR requires evidence of graft dysfunction (e.g., elevated aminotransferases), typically followed by confirmation via allograft biopsy, which is considered the best method (4). In addition, the interpretation of liver biopsies can be challenged because of the frequent absence of the classic features of the portal triad (5, 6). Endotheliitis has been reported in up to 60% patients with hepatitis C infection (7). The majority of these episodes (~85%) are resolved with antirejection treatment (commonly pulses of systemic corticosteroids), but induction of graft acceptance may be disturbed as the same time (3). Acute rejection and acceptance induction remain critical issues in relation to prognosis after LTx. Therefore, there is an urgent unmet need for the effective strategies of diagnosis and therapy after LTx.

Cellular, humoral, and complement components are involved in AR of liver allograft and exert their effects through the peripheral circulation (8). Serum components may include useful biomarkers associated with the immune response of liver allograft, which could be used to predict outcomes especially at the early stages (9, 10). In general, proteomic analysis provides a better understanding of biological processes than genomics because proteomics avoids the effects of rapid degradation or inefficient translation of mRNA, posttranslational modifications, and functional changes generated from complexes with other proteins or RNA molecules (11, 12).

Proteomic approaches have been largely applied to studying of bone marrow (13, 14), renal (15, 16), cardiac (17), and

Address reprint requests to Jia Fan, MD, PhD, Liver Cancer Institute, Zhongshan Hospital, Fudan University, 180 Feng Lin Rd, Shanghai, China 200032. E-mail: jiafan99@yahoo.com.; or Xiaowu Huang, MD, PhD, Liver Cancer Institute, Zhongshan Hospital, Fudan University, 180 Feng Lin Rd, Shanghai, China 200032. E-mail: huang.xiaowu@zs-hospital.sh.cn.

Min Xu, Changjun Tan, and Jinwu Hu contributed equally to this work.

This study was supported by the National Natural Science Fund of China (grant nos. 30700815, 81272724, and 81225019), by the Major Program of NSFC (grant no.81030038), by the National Key Sci-Tech Special Project of China (grant no. 2012ZX10002-016), and by the Natural Science Foundation of Shanghai City (grant no. 13ZR1406900).

Fan J and Huang X conceived and designed the experiments; Xu M, Tan C, and Hu J performed the experiments; Xu M analyzed the data; Yan J, Hu J, Dai Z, Wang Z, and Zhou J contributed reagents/materials/analysis tools; and Xu M and Alwahsh SM were responsible for writing and critical improvement of the manuscript.

The authors declare that no competing interests exist.

DOI: 10.1097/SHK.0000000000000171

pulmonary transplantations (18, 19). Haptoglobin is a typical hemoglobin-binding protein that inhibits hemoglobin oxidation. Using traditional two-dimensional gel electrophoresis analysis, Pan et al. (20) reported upregulation of haptoglobin in a tolerant rat liver allograft. The group proposed that haptoglobin promotes tolerance after LTx via inhibiting T-cell proliferation (20). Two-dimensional gel electrophoresis and mass spectrometry (MS) additionally used to investigate proteomic differences between rejected and accepted liver grafts have provided valuable clues about the dysfunction of graft undergoing AR (21). Further proteomic analyses disclosed that serum C4 and alanine transaminase levels are highly predictive of AR in liver transplant recipients (22).

Given that AR and acceptance of liver allograft are critical issues for further improvement of prognosis after LTx, effective analyses are essential. With the aim of exploring potential changes in serum proteins in allograft rejection recipients, rat LTx was performed (from Lewis to Brown Norway [BN]), and the severity of graft rejection was graded by the Banff schema. Subsequently, biomarkers in rat serum were detected using two-dimensional difference gel electrophoresis (2D-DIGE) and mass spectrographic analyses. The biomarkers identified were further validated in other rat models with AR or acceptance after LTx and *in vitro* lymphocyte culture studies.

MATERIALS AND METHODS

Animals

Male Lewis, BN, and F344 inbred rats weighting 220 to 250 g were obtained from Peking Vital River Laboratory Animal Ltd, and August Copenhagen Irish (ACI) inbred rats were purchased from Harlan Laboratory Ltd. Rats were given standard chow diet and water and housed in laminar flow cages under specific pathogen–free conditions at Zhongshan Hospital of Fudan University (Shanghai, China). Animals received humane care according to the criteria outlined in the Guide for the Care and Use of Laboratory Animals recommended by the National Academy of Sciences. All procedures in this study were approved by the Council of Animal Care in Fudan University.

Rat LTx and experimental design

Rats were anesthetized with isoflurane (2% – 5% with oxygen flow 1.5 to 2 L/min) during the operation. A daily dose (5 mg/kg) of ketoprofen was subcutaneously administrated to relieve pain until day 5 after rat LTx. Recipient rats were rewarmed for 12 h under a heating lamp. Rat LTx was performed using Kamada two-cuff method without reconstruction of the hepatic artery (23). Liver grafts of male Lewis rats (donors) were transplanted to BN rats, and the recipients were sacrificed between days 5 and 15 after LTx. Hematoxylin and eosin (HE) sections of rat liver were independently evaluated by three pathologists, and the Rejection Activity Index ((RAI), composed of three components scored from 0 to 3, specifically, venous endothelial inflammation (E), bile duct damage (B), and portal inflammation (P), was calculated according to the Banff schema. Subsequently, rat liver allografts were categorized into control (no evidence of rejection), mild, moderate, and severe acute cellular rejection (AR) groups (n = 3 per group) (24). To validate results obtained from the Lewis to BN rat combination, we additionally performed LTx from Lewis to ACI, BN to ACI, and F344 to ACI rats (n = 3 per group). Concomitantly, syngeneic LTx from male BN to BN or ACI to ACI rats served as controls (n = 3 per group). Liver and serum samples were harvested from all recipients for biological analysis.

Histological studies

Liver grafts were harvested and fixed in 10% buffered formalin or snap-frozen in liquid nitrogen. Fixed livers were embedded in paraffin, sectioned serially at 4-μm thickness, de-waxed, and stained with HE. All HE-stained sections were examined in a blind manner by three different pathologists, and images were obtained under a light microscope (Leica Corporation) at a magnification of 200×. Rejection activity (Lewis to BN) was scored and graded using the Banff schema as previously mentioned. Based on categorization (control, mild, moderate, or severe rejection), three samples from each group were selected for proteomic and other analyses.

2D-DIGE analysis

A 100-μg aliquot of protein from each animal of the control, mild, moderate, and severe AR groups was subjected to 2D-DIGE analysis (Lewis to BN; n = 3 per group). High-abundance proteins of BN recipient serum were depleted using the Multiple Affinity Removal System (MARS; Agilent Technologies, Santa Clara, Calif). Subsequently, 4.2 μg protein of each sample was mixed together and labeled with Cy2, served as the internal standard. Overall, 12 samples were randomly labeled with Cy3 or Cy5. An aliquot (50 μg) of each sample was loaded in the well of the gel (two samples per gel). Two-dimensional DIGE analysis was performed as described previously (25, 26). Gel analysis was performed using DeCyder 2D 5.0 software (GE Healthcare) applying the biological variation analysis module to allow the comparison of spot ratios between all gels by matching the internal standard images. After the match of the standard spots map, changes in protein abundance were statistically analyzed using the DeCyder Biological Variation Analysis software.

MS and database searching

Spots with significant changes in average intensity among different maps were selected for identification using MS. Matrix-assisted laser desorption/ionization time-of-flight (MALDI-TOF)/TOF MS spectra were searched using the mascot database under a combined mode (MS plus MS/MS) with the following parameters: trypsin specificity, one missed cleavage, cysteine carbamidomethylation and methionine oxidation as variable modifications, peptide tolerance at 0.2 Da, and MS/MS tolerance at 0.25 Da. Linear trap quadrupole (LTQ) MS spectra were searched using the IPI RAT v3.36 database under the following Xcorr criteria: greater than 1.5 for singly charged ions, Xcorr greater than 2.0 for doubly charged ions, and Xcorr greater than 2.5 for triply charged ions. Peptide tolerance of ±2 Da and MS/MS tolerance of ±1 Da were allowed.

Serum study with enzyme-linked immunosorbent assay sandwich

Blood specimens from all recipient rats were collected via BD Vacutainer coated with silicones promoting coagulation and centrifuged at 3,000 rpm for 10 min within 1 h after collection. Sera were stored at −80°C until use. To validate the results obtained with proteomic analysis, protein concentrations of hemopexin (HPX), complement C3 (C3), and kininogen were determined using commercial Rat HPX, C3 enzyme-linked immunosorbent assay (ELISA) kits (GenWay Biotech, Inc), and kininogen ELISA kits (Cusabio Biotech, Co, Ltd), respectively. The concentrations of interferon-γ ([IFN-γ] RIF00; R&D), interleukin 17 ([IL-17] E90063Ra; Uscn Life Science), and IL-10 (R1000; R&D) were additionally detected with ELISA. All procedures were performed in keeping with the supplier's protocol. Samples were analyzed in triplicate, and standard curves were generated according to the manufacturer's instructions. A four-parameter standard curve was constructed using Curve Expert Version 1.3 software.

Western blots

As reported previously (27), Western blot analysis was performed with 50 μg of cytosolic protein from graft liver tissues (Lewis to BN). After blocking nonspecific binding with nonfat dry milk, membranes were incubated overnight at 4°C with mouse monoclonal antibodies for RAT HPX (SantaCruz). Blots were incubated with secondary goat anti-mouse antibody (1:10,000; Pierce Chemical, Rockford, Ill) for 1 h at room temperature. Signals were developed with the Super Signal West Femto Maximum Sensitivity Substrate detection systems (Pierce Chemical) and subsequently exposed to film. Nicotinamide adenine dinucleotide phosphate was used as the loading control. Band intensities were measured with ImageJ software 1.46 (developed by the National Institutes of Health).

Isolation and culture of lymphocytes

Spleens of Lewis and BN rats were harvested and homogenized, and tissue fractions passed through a nylon cell strainer (70 μm) to remove debris. Cultures were incubated in an atmosphere consisting of 7% O_2, 10% CO_2, and 83% N_2 at 37°C. The cell suspension was transferred to lymphocyte separation medium (TBD, LTS1083P; 1:1 volume). The white blood cell phase was isolated via density gradient centrifugation (1,600 rpm, 20 min), incubated in RPMI1640 (cat 11875093; Gibco), and centrifuged at 1,600 rpm for 8 min. Cells were resuspended and seeded in 24-mL culture flasks, followed by incubation at 37°C for 1 h. The Lewis rat cell suspension was transferred to new centrifuge tubes, treated with 25-μg/mL mitomycin-C (M7949-2MG; Sigma), and incubated for 1 h at 37°C. To deplete mitomycin-C suspensions were centrifuged three times at 1,600 rpm for 8 min.

Mixed lymphocyte reaction and stimulation with HPX

Lymphocytes from Lewis (mitomycin-C treated) and BN rats were suspended in RPMI1640, counted, and diluted at a concentration of 5×10^6/mL. Subsequently, 100-μL cell suspensions of Lewis and BN rat were cocultured

in 96-well plates. Mixed cells were stimulated with HPX protein (H9291; Sigma) at the following concentrations: 0 (control), 0.03, 0.08, 0.3, 0.83 μM (n = 3 for each dose, repeated three times). An equivalent concentration of BN rat cell suspension served as the negative control. All cells were incubated at 37°C for 72 h. A 22-μL aliquot of CCK-8 (C0038; Beyotime Inst Biotech) was added to each well 1 h before subjected to measurement in a microplate reader (450 nm). Subsequently, absorbance (optical density [OD]) was recorded. The proliferation rate was calculated as OD (HPX treated)/OD (control) ×100%. Separate plates subjected to the same were used to measure IFN-γ (50 μL), IL-17 (100 μL), and IL-10 (50 μL) concentrations in supernatants collected using ELISA.

Reverse transcription and real-time polymerase chain reaction

Total RNA was extracted from liver tissue (Lewis to BN) using a Total RNA Isolation Kit (Invitrogen Life Technologies). Oligonucleotides were designed with Primer Express software (Applied Biosystems, Foster City, Calif) as follows: *Hpx* forward: 5′-CTG CCT CAG CCC CAG AAA GT-3′, reverse: 5′-GGG TGG GCT GGG CTA ATT C-3′; metallothionein (*Mt-1*) forward: 5′-CAA ATG CAC CTC CTG CAA GA-3′, reverse: 5′-CTG CTC CAA ATG TGC CCA GGG CT-3′; heme oxygenase-1 (*Ho-1*) forward: 5′-CTT GCA GAG AGA AGG CTA CAT GA-3′, reverse: 5′-AGA GTC CCT CAC AGA CAG AGT TT-3′; ferritin l-chain (*Ftl*) forward: 5′-CTA CCT CTC TCT GGG CTT CT-3′, reverse: 5′-GGT TGG TCA GGT GGT TGC CC-3′; ferritin h-chain (*Fth*) forward: 5′-TGA CAA GAA TGA TCC CCA C-3′, reverse: 5′-CTT AGC TCT CAT CAC CGT GT-3′; proliferating cell nuclear antigen (*Pcna*) forward: 5′-TTT GAG GCA CGC CTG ATC C-3′, reverse: 5′-GGA GAC GTG AGA CGA GTC CAT-3′; *Il-10* forward: 5′-CCA TTC CAT CCG GGG TGA CA-3′, reverse: 5′-TTT CTG GGC CAT GGT TCT CTG C-3′; *Ifn-γ* forward: 5′-GCC AAG TTC GAG GTG AAC AAC-3′, reverse 5′-TAG ATT CTG GTG ACA GCT GGT GAA-3′; and *Il-17* forward: 5′-ATC AGG ACG CGC AAA CAT G-3′, reverse: 5′-TGA TCG CTG CTG CCT TCA C-3′. Gene expression was normalized by *Gapdh* (housekeeping gene: forward primer: 5′-GGA AAG CTG TGG CGT GAT-3′, reverse primer: 5′-AAG GTG GAA GAA TGG GAG TT-3′. Real-time polymerase chain reaction was performed in a final reaction volume of 10 μL containing complementary DNA from reverse-transcribed total RNA, 150 nM forward and reverse primers, and SybrGreen universal PCR master mix (Applied Biosystems) on the ABI 7900 RT-PCR Apparatus (Applied Biosystems). All reactions were performed in triplicate. Melting curve analysis was performed, and dilution curve standards were generated.

Statistical analysis

Data were statistically analyzed using GraphPad Prism 4 software (San Diego, Calif) and SPSS statistical package (SPSS 12.0 for windows, Chicago, Ill). One-way analysis of variance was used for examining the statistical differences among groups in a proteomic study. The Student *t* test was applied to compare differences between the two groups. Data are expressed as means ± SEM. Differences were accepted as significant at $P < 0.05$.

RESULTS

To explore the changes in serum biomarkers during acute rejection of rat liver graft, Lewis rat livers were transplanted into BN recipient rats. Animals were divided into mild, moderate, and severe rejection groups according to the Banff schema;

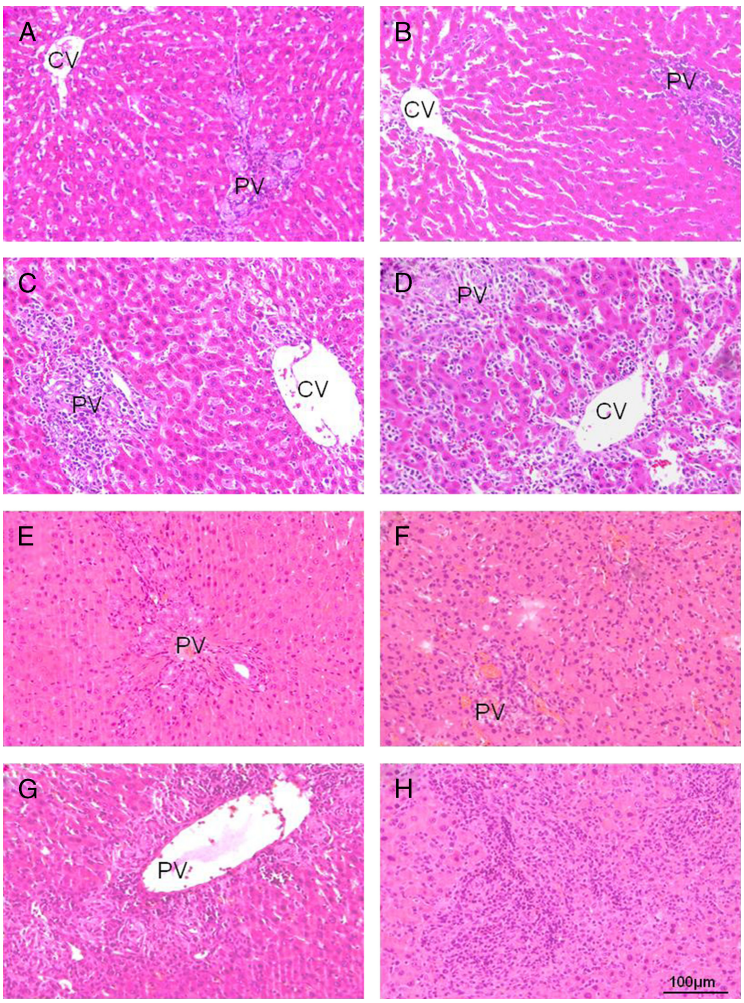

FIG. 1. **Histological manifestation of liver grafts (HE staining)**. Representative micrographs of HE-stained livers show the following: A, BN to BN rat syngeneic control group, no evidence of rejection. B, Lewis to BN rat LTx with mild AR of liver allograft. C, Lewis to BN rat LTx with moderate AR of liver allograft. D, Lewis to BN rat LTx with severe AR of liver allograft. E, ACI to ACI rat syngeneic control, no sign of AR. F, BN to ACI LTx, spontaneous acceptance. G, Lewis to ACI LTx, alterations in AR. H, F344 to AC LTx, presenting changes of AR. AR indicates acute rejection; CV, central vein; PV, portal vein. Scale bar: 100 μm.

BN to BN rat LTx served as the syngeneic control. Other rat LTx models (Lewis, F344, BN, and ACI to ACI rats) were additionally investigated (n = 3 per group) to validate the results obtained. Changes in serum biomarkers were studied using 2D-DIGE + MS, ELISA, RT-PCR, and Western blotting analyses. Lymphocytes from BN spleen were isolated and treated with HPX to determine the functions of representative protein.

Histological manifestations

No sign of AR was observed in liver graft sections of BN to BN rats (control), whereas allografts of Lewis to BN rats displayed mild, moderate, or severe AR, as assessed with the Banff schema (Fig. 1, A–D). In addition, no indication of rejection was observed in the liver graft of ACI to ACI (Fig. 1E) and BN to ACI rats (spontaneous tolerance; Fig. 1F). In contrast, liver sections of Lewis to ACI and F344 to ACI rats presented clear AR (Fig. 1, G–H).

Changes in serum protein levels according to severity of AR

In the combination of Lewis to BN LTx, protein samples extracted from recipient serum were analyzed using 2D-DIGE. Representative images are shown in Figure 2, A–D. Expression of 30 protein spots (Fig. 2E) was significantly altered among syngeneic control, mild, moderate, and severe rejection groups ($P < 0.01$; details in Tables 1 – 2).

MS/MS identification of serum proteins

In total, 30 spots were selected for protein identification using MALDI-TOF or LTQ MS/MS. Sixteen spots were identified with MALDI-TOF MS/MS (Table 1) and others with LTQ MS/MS (Table 2). The relevant parameters are additionally listed in the respective tables. Finally, 14 serum biomarkers were identified after the exclusion of repetitive proteins. In particular, five spots of interest were identified as HPX. The standard log abundance changes of representative proteins are presented in Figure 3. Based on biological functions, the specified proteins were categorized as follows: 1) metabolic immunoregulators, including HPX (Fig. 3A), preprohaptoglobin ([PHp] Fig. 3B), Srprb Ba1-667, and preproapoA-I; 2) components related to innate immune response, containing C3 complement ([C3] Fig. 3C), mannose-binding protein (MBP-A; Fig. 3D), C4a complement, LOC500183 protein, and LOC299458 protein; 3) immunoregulatory polypeptides, including T-kininogen 2 ([KNG] Fig. 3E), alpha-1-macroglobin (α1-M) (Fig. 3F), and chain A crystal structure of rat α1-M receptor–binding domain; 4) other proteins ORF2 and rCG36664.

Levels of HPX, C3, and KNG in recipient serum

The concentrations of HPX, C3, and KNG in recipient serum were detected with ELISA. As shown in Figure 4A (Lewis to BN), HPX protein levels in serum were significantly reduced in mild, moderate, and severe AR groups than that in the control group (*$P < 0.05$, respectively). As shown in Figure 4B, serum HPX levels were significantly decreased in other independent rejection combinations (Lewis or F344 to ACI) relative to the syngeneic control group (ACI to ACI, *$P < 0.05$). Compared with the control group, the HPX protein level of the tolerant group (BN to ACI) presented no remarkable changes. Conversely, serum levels of C3 in moderate and severe AR (Lewis to BN) as well as in Lewis/F344 to ACI groups were significantly increased compared with syngeneic control (Fig. 4, C and D; *$P < 0.05$, respectively). In addition, KNG protein levels of Lewis to BN/ACI groups were significantly downregulated compared with those in the control (Fig. 5, E and F; *$P < 0.05$, respectively). Indeed, the significant changes in C3, C4, and haptoglobin were particularly presented as the previous studies reported (20, 22). Our study highlighted a set of novel biomarkers, including HPX, KNG, MBP-A, and α1-M.

Expression of the HPX *gene in rat liver grafts (Lewis to BN)*

To evaluate HPX gene expression in liver grafts (Lewis to BN), RT-PCR and Western blotting analyses were applied. As shown in Figure 5A, *Hpx* mRNA expression was significantly reduced in the moderate and severe AR groups compared with the control group ($P < 0.05$). Densitometric analysis of Western blots (Fig. 5B) revealed similar results (Fig. 5C; *$P < 0.05$).

Transcription levels of Mt-1, Ho-1, Fth, *and* Ftl *in isolated rat lymphocytes stimulated with HPX*

As shown in Figure 6, A and B, *Mt-1* (20-fold) and Ho-1 (5-fold) mRNA levels were significantly elevated (0.3 μM) in

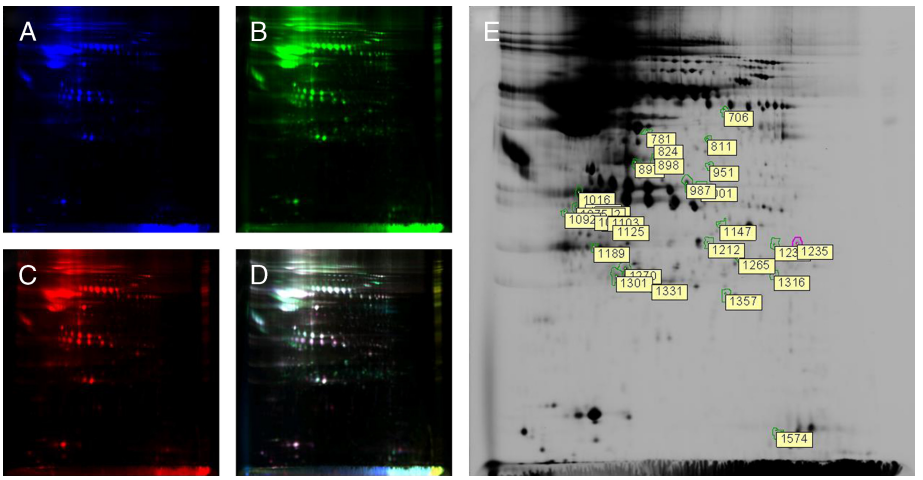

Fig. 2. **Representative images of 2D-DIGE analysis**. A, Mixed protein samples (4.2 μL from each animal) labeled with Cy2 served as the internal standard. B and C, Samples were randomly labeled with either Cy3 or Cy5. D, Overlap of Cy2, 3, 5-labeled Channel (Lewis to BN LTx, n = 3 for control, mild, moderate, and severe AR groups, respectively). E,) Localization of 30 protein spots with significantly altered abundance in the gel.

TABLE 1. **The serum proteins identified by MALDI-TOF/TOF MS/MS in liver allograft rejection**

Spot no.	Protein name	NCBI entry	Theoretical MW (cal)(D)	*P*	p*I* (cal)	Peptide matches	Sequence coverage, %	Protein score
951	Complement C3	gil116597	187825	0.002	6.12	14	10	77
1001	Hemopexin, isoform CRA_c	gil149068484	28927	0.008	6.09	6	19	63
1092	Hemopexin; Flags: Precursor	gil122065203	52060	0.004	7.58	9	16	81
824	rCG36664	gil149019925	48812	0.004	6.03	3	6	106
897	Complement component C3	gil554423	32414	0.008	5.73	3	16	166
898	Complement component C3	gil554423	32414	0.01	5.73	4	21	151
987	Chain A, Crystal Structure of Rat Alpha 1-Macroglobulin Receptor Binding Domain	gil12084772	15354	0.01	5.78	3	27	93
1050	Hemopexin; Flags: Precursor	gil122065203	52060	0.001	7.58	3	9	179
1059	Preprohaptoglobin	gil204657	30428	0.001	7.16	3	12	149
1072	Hemopexin; Flags: Precursor	gil122065203	52060	0.001	7.58	3	8	101
1075	Hemopexin	gil16758014	52000	0.01	7.58	2	4	118
1097	Preprohaptoglobin	gil204657	30428	0.003	7.16	5	16	224
1098	Preprohaptoglobin	gil204657	30428	0.002	7.16	3	12	147
1103	ORF2	gil202959	38359	0.008	5.89	4	13	96
1265	Preprohaptoglobin	gil204657	30428	0.007	7.16	4	14	167
1331	Preproapolipoprotein A-I	gil55747	30126	0.01	5.52	1	4	51

HPX-treated lymphocytes compared with nontreated lymphocytes (**P* < 0.05, respectively). In comparison with the nontreated group, marginally significant *Fnh* mRNA changes (**P* < 0.05), but no changes in *Fnl* mRNA expression (Fig. 6, C and D), were observed.

Transcriptional changes in cytokines in HPX-treated rat lymphocytes

We observed a 1.5-fold increase in *Pcna* mRNA level at a dose of 0.3 μM HPX (Fig. 7A; **P* < 0.05). Expression of *Il-10* mRNA was lower in HPX-treated lymphocytes (0.83 μM) compared with nontreated lymphocytes (Fig. 7B; **P* < 0.05). Relative to the nontreated group, Ifn-γ (6.5-fold; 0.3 μM) and Il-17 (3-fold; 0.83 μM) mRNA levels were significantly elevated (Fig. 7, C – D; **P* < 0.05).

In vitro *effect of HPX on growth of rat lymphocytes in MLR*

At 72 h after HPX delivery, the proliferation rate of lymphocytes (treated with 0.83 μM HPX) was marginally decreased compared with that in nontreated cells (**P* < 0.05; Fig. 8A).

TABLE 2. **The serum proteins identified by LTQ MS/MS in liver allograft rejection**

Spot no.	Protein name	IPI accession no.	Theoretical MW (cal)(D)	*P*	p*I* (cal)	Peptide matches	Sequence coverage, %
1016	C3 Complement C3 precursor (Fragment)	IPI00480639.3	186460	0.005	6.12	9	5.05
1125	C3 Complement C3 precursor (Fragment)	IPI00480639.3	186460	0.005	6.12	6	3.61
1147	C4a Complement C4 precursor	IPI00213036.4	192163	0.005	6.99	3	1.55
1189	Pzp Alpha-1-macroglobulin precursor	IPI00326140.3	167125	0.006	6.46	4	2.47
1232	Srprb Ba1-667	IPI00196656.2	107226	0.002	8.35	2	2.14
1235	Mbl1 Mannose-binding protein A precursor	IPI00325371.1	25308	0.001	7.54	6	21.43
1270	LOC500183 protein	IPI00568389.2	25692	0.008	5.34	3	17.09
1301	LOC500183 protein	IPI00568389.2	25692	0.007	5.34	6	23.93
1316	LOC500183 protein	IPI00568389.2	25692	0.005	5.34	3	17.09
1574	MGC108747 T-kininogen 2 precursor	IPI00558996.2	47704	0.007	5.98	2	3.72
706	Srprb Ba1-667	IPI00196656.2	107225	0.001	8.35	3	3.06
781	C3 Complement C3 precursor (Fragment)	IPI00480639.3	186460	0.002	6.12	8	5.35
811	LOC299458 protein	IPI00368874.2	65920	0.003	6.33	4	6.86
1212	MGC108747 48 kd protein	IPI00558996.2	47928	0.002	5.98	5	9.26

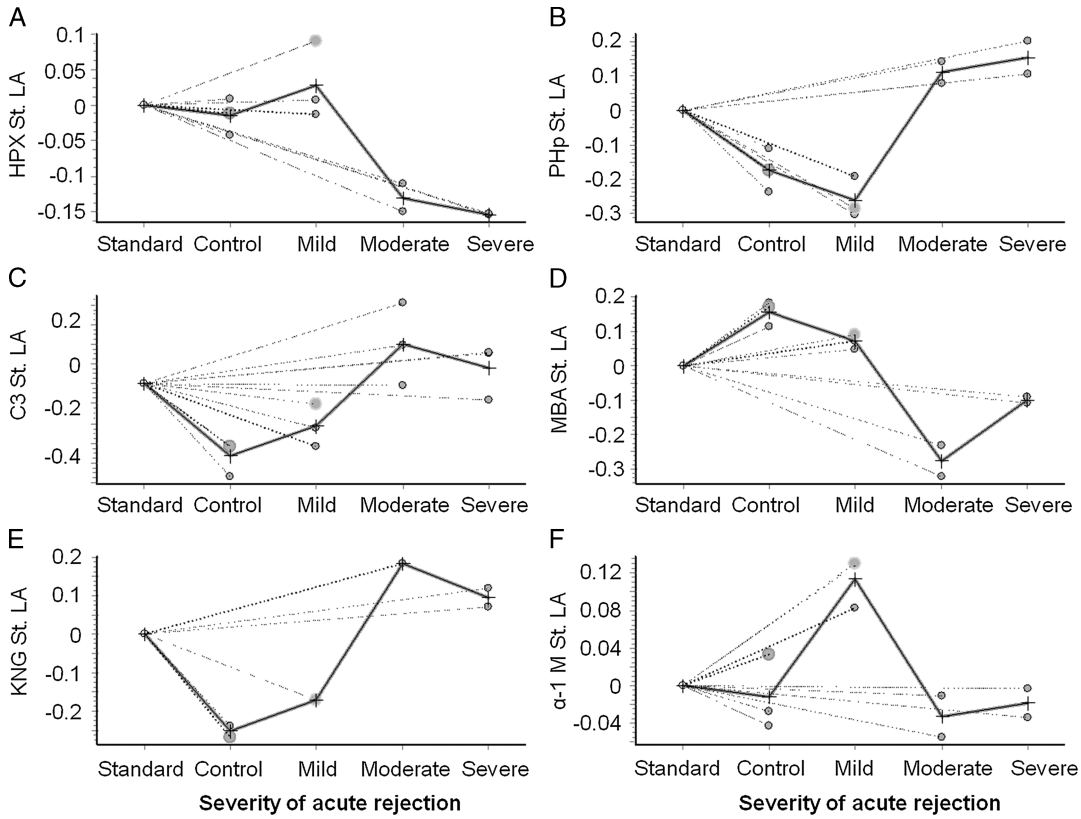

Fig. 3. **Standard log abundance changes of representative biomarkers**. In the combination of Lewis to BN LTx (mild, moderate, severe AR, BN to BN LTx served as control, n = 3 per group), standard log abundance (St.LA) changes of representative proteins were presented, including HPX (A), PHp (B), C3 (C), MBP A (D), KNG (E), and α1-M (F). One-way analysis of variance, $P < 0.05$.

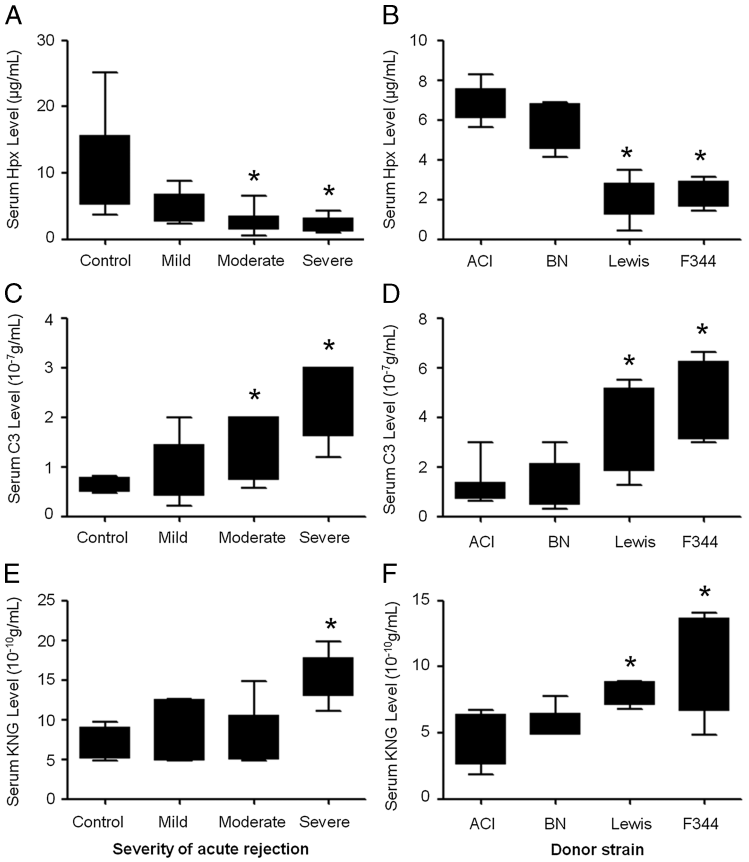

Fig. 4. **Validation of representative biomarkers with ELISA**. Serum HPX (A), C3 (C), and KNG (E) levels of BN recipients (Lewis donor). The X-axis represents the histological findings of liver graft. Serum HPX (B), C3 (D), and KNG (F) levels of ACI recipients (ACI, BN, Lewis, and F344 donors). The X-axis represents donor strains (n = 3 per group; $^*P < 0.05$).

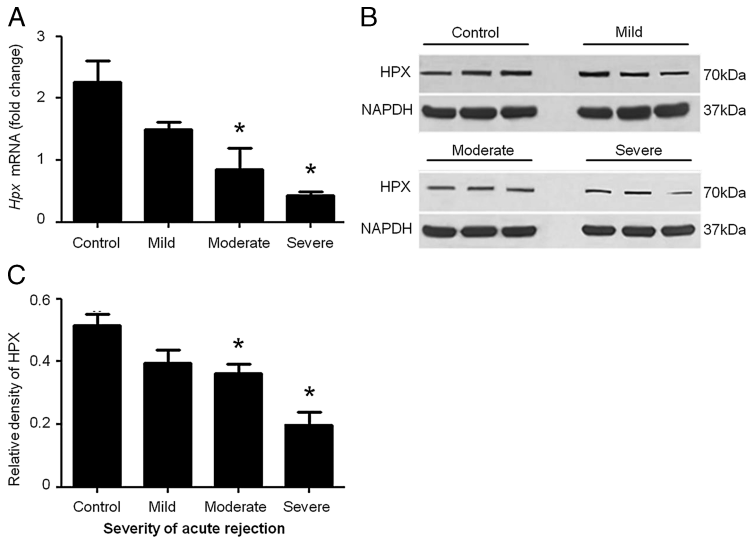

FIG. 5. **Gene expression of HPX in rat liver grafts (Lewis to BN)**. Expression of HPX was analyzed at both the RNA and protein levels. A, Hepatic *Hpx* mRNA was detected with RT-PCR. B, Determination of HPX protein expression using Western blot. Nicotinamide adenine dinucleotide phosphate served as internal standard. C, Densitometric analysis for HPX protein in rat livers (n = 3 per group; $^*P < 0.05$).

Compared with untreated cells, mild alterations in proliferation rate were observed at doses of 0.03, 0.08, and 0.3 μM HPX.

HPX promotes IFN-γ and IL-17 and decreases IL-10 synthesis in rat lymphocytes

As shown in Figure 8B, HPX treatment at all selected doses led to a significant increase in IFN-γ synthesis compared with the untreated group ($^*P < 0.05$). Stimulation of lymphocytes with 0.83 μM HPX led to increased IL-17 (Fig. 8C) and decreased IL-10 levels (Fig. 8D) compared with control in the MLR trial ($P < 0.05$).

DISCUSSION

In the current study, a proteomic signature for AR of rat liver allograft was identified using 2D-DIGE and MS analyses. In total, 14 proteins in sera were isolated after the exclusion of repetitive spots. Unexpectedly, five protein spots of interest in the gels were repeatedly identified as HPX protein, indicating a critical role in AR of rat liver allograft. Hemopexin mRNA and protein levels in liver allograft presented descending trends in relation to AR severity. Furthermore, *in vitro* treatment with HPX significantly affected the expression of metal metabolism–related and cytokine genes in isolated lymphocytes.

Hemopexin, a 60-kDa positive acute-phase plasma β1-glycoprotein that binds heme, is released into the blood as a result of hemolysis or rhabdomyolysis and transports heme principally to the liver (28–30). Hemopexin is mainly expressed in the liver and displays the highest affinity to heme (K_d, <1 pM) (31). In a study on cold-preserved liver, HPX inhibited heme-mediated cellular injury and oxidative damage to rat liver graft by forming a complex with heme (32). In the present investigation,

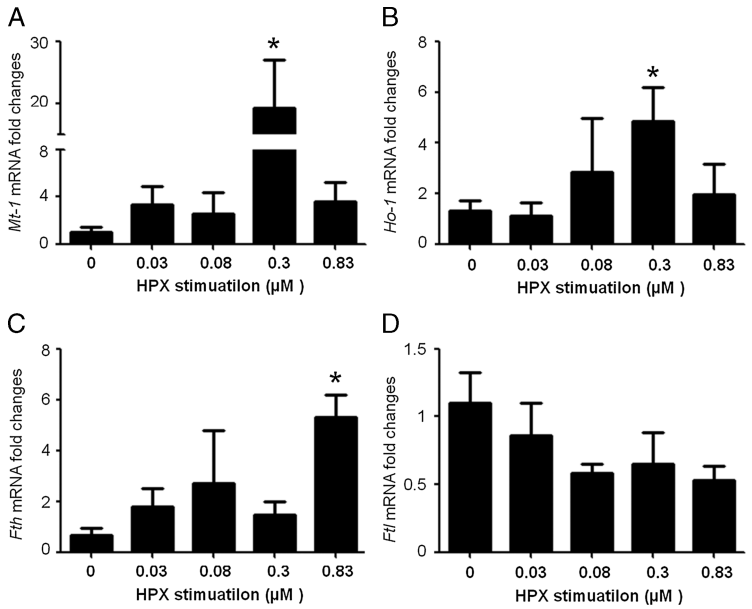

FIG. 6. **Expression of *Mt-1, Ho-1, Fth,* and *Ftl* mRNA in rat lymphocytes**. Isolated lymphocytes were stimulated with different doses of HPX. *Mt-1* (20-fold) and *Ho-1* (5-fold) mRNA levels were significantly elevated (0.3 μM) in HPX-treated lymphocytes compared with untreated lymphocytes. Compared with the nontreated group, marginal significance of Ferritin H (*Fnh*) mRNA expression was observed. *Gapdh* served as a housekeeping gene ($^*P < 0.05$).

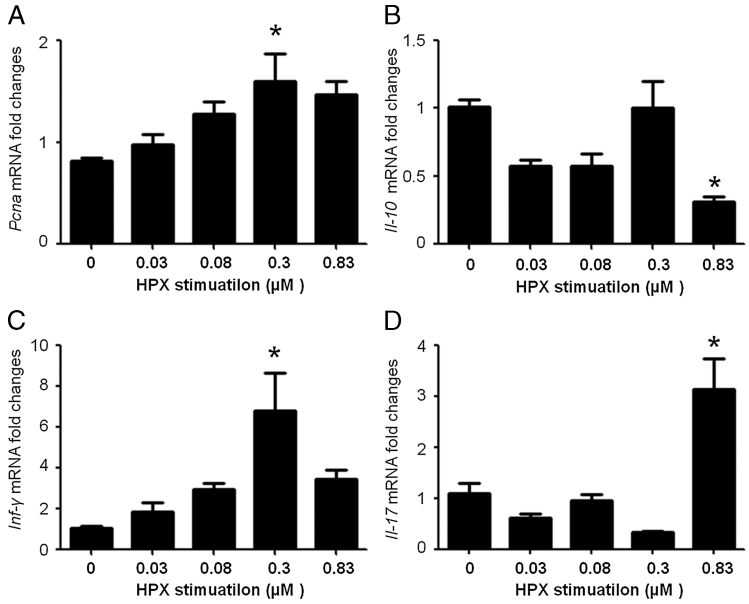

Fig. 7. **Expression of *Pcna, Il-10, Ifn-γ,* and *Il-17* mRNA in rat lymphocytes**. We observed 1.5-fold upregulation of *Pcna* mRNA at a dose of 0.3 μM HPX (A). Expression of *Il-10* mRNA was significantly lower in HPX-treated lymphocytes (0.83 μM) than that in untreated lymphocytes (B). Compared with the untreated group, *Ifn-γ* (6.5-fold; 0.3 μM) and *Il-17* (3-fold; 0.83 μM) mRNA levels were significantly elevated. *Gapdh* served as the housekeeping gene (C, D; **P* < 0.05).

we observed a significant decrease in HPX levels in both sera and liver allograft with AR (Lewis to BN, Lewis or F344 to ACI) but no remarkable changes in the tolerant recipient (BN to ACI), indicating a negative correlation between HPX expression and AR of rat liver allograft. The gene levels of *Mt-1* and *Ho-1* in rat lymphocytes are upregulated after stimulation with HPX *in vitro*. These findings suggest that upregulation of MT-1 enhances cellular resistance to oxidative stress, and that MTs are capable of iron binding in an acidic and reducing lysosomal-like environment (33). Upregulation of HO-1 has been proposed as an adaptive mechanism protecting against hepatic ischemia/reperfusion injury (34). In addition, HPX plays an inhibitory role in neutrophil migration during sepsis (35), suggesting that HPX therapy reduces recruitment of neutrophils to the liver allograft. In view of the collective findings, we suggest that HPX protects rat liver allograft against injuries.

Hemopexin heme may serve as a source of iron and consequently promote the proliferation of acute T-lymphoblastic cells (36, 37). Hemopexin heme and heme are proposed natural substrates for growth-associated electron transfer across the plasma membrane (38). In our study, *Pcna* was significantly upregulated in rat lymphocytes after stimulation with HPX at a dose of 0.3 μM, suggesting a positive role of HPX in cell proliferation. However, only a marginal decrease in the

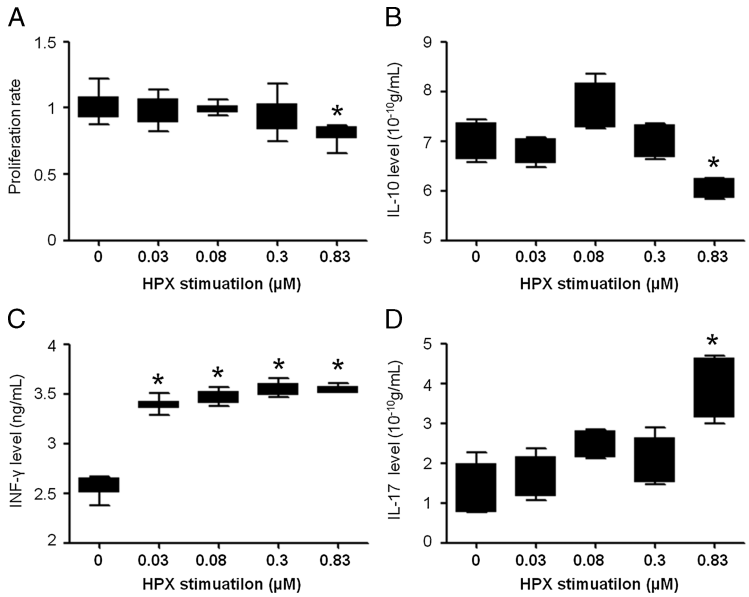

Fig. 8. **Lymphocyte proliferation and IL-10, IFN-γ, and IL-17 concentrations**. Lymphocyte proliferation rate, calculated as OD (HPX-treated)/OD (control) ×100%, was marginally decreased in the MLR trial (A). Enzyme-linked immunosorbent assay analysis of IL-10 (B), IFN-γ (C), and IL-17 (D) concentrations in lymphocyte supernatants treated with different doses of HPX (**P* < 0.05 compared with control, 0 μM).

lymphocyte proliferation rate was observed at a dose of 0.83 μM HPX, and no significant changes were evident at other doses. This could be explained by the theory that at an extreme high dose of HPX either competitively bound to its receptor, leading to low effectiveness usage of iron (essential for cell growth), or manifested a toxic effect.

Serum HPX level and AR severity were negatively correlated in our experiments. Moreover, treatment of rat lymphocytes with HPX significantly increased the IFN-γ and IL-17 levels in the supernatant of cultured lymphocytes, and IL-10 expression was significantly downregulated. Analysis of a human acute T-lymphoblastic cell line treated with HPX indicated that HPX heme not only functions as an iron source for T cells but also occupies the HPX receptor itself, triggering signaling pathways related to regulation of cell growth (36). As reported previously, lack of HPX inhibited mercury-induced autoimmune responses in mice through controlling heme iron availability in lymphocytes, modulated responsiveness to IFN-γ. Compared with wild-type mice, $CD4^+$ T cells isolated from mercury-treated HPX-null mice showed reduced IFN-γ–dependent STAT1 phosphorylation (39). Hemopexin not only protects liver allografts against oxidative injury but also promotes acceptance of liver graft. The animal number of each group for proteomics analysis is limited because of the expensive cost. Further studies, particularly *in vivo* with interventions, are clearly required to improve our understanding of the role of HPX in AR of liver allograft.

In conclusion, the current findings facilitated the generation of a serum proteomic profile of rat liver AR. Our results collectively indicate that HPX serves as a negative predictor for AR of liver allograft. Furthermore, treatment with HPX *in vitro* may regulate cytokine expression.

ACKNOWLEDGMENTS

The authors thank Mr. Hou C for technical help.

REFERENCES

1. Shaked A, Ghobrial RM, Merion RM, Shearon TH, Emond JC, Fair JH, Fisher RA, et al.: Incidence and severity of acute cellular rejection in recipients undergoing adult living donor or deceased donor liver transplantation. *Am J Transplant* 9:301–308, 2009.
2. Klintmalm GB, Washburn WK, Rudich SM, Heffron TG, Teperman LW, Fasola C, Eckhoff DE, et al.: Corticosteroid-free immunosuppression with daclizumab in HCV(+) liver transplant recipients: 1-year interim results of the HCV-3 study. *Liver Transpl* 13:1521–1531, 2007.
3. Wiesner RH, Demetris AJ, Belle SH, Seaberg EC, Lake JR, Zetterman RK, Everhart J, et al.: Acute hepatic allograft rejection: incidence, risk factors, and impact on outcome. *Hepatology* 28:638–645, 1998.
4. Demetris A, Adams D, Bellamy C, Blakolmer K, Clouston A, Dhillon AP, Fung J, et al.: Update of the International Banff Schema for Liver Allograft Rejection: working recommendations for the histopathologic staging and reporting of chronic rejection. An International Panel. *Hepatology* 31:792–799, 2000.
5. Regev A, Molina E, Moura R, Bejarano PA, Khaled A, Ruiz P, Arheart K, et al.: Reliability of histopathologic assessment for the differentiation of recurrent hepatitis C from acute rejection after liver transplantation. *Liver Transpl* 10: 1233–1239, 2004.
6. Sawada T, Shimizu A, Kubota K, Fuchinoue S, Teraoka S: Lobular damage caused by cellular and humoral immunity in liver allograft rejection. *Clin Transplant* 19:110–114, 2005.
7. Thuluvath PJ, Krok KL: Noninvasive markers of fibrosis for longitudinal assessment of fibrosis in chronic liver disease: are they ready for prime time? *Am J Gastroenterol* 101:1497–1499, 2006.
8. Brent LB: The immunobiology of transplantation. *Int Surg* 84:275–278, 1999.
9. Hariharan S, Kasiske B, Matas A, Cohen A, Harmon W, Rabb H: Surrogate markers for long-term renal allograft survival. *Am J Transplant* 4:1179–1183, 2004.
10. ter Meulen CG, Jacobs CW, Wetzels JF, Klasen IS, Hilbrands LB, Hoitsma AJ: The fractional excretion of soluble interleukin-2 receptor-alpha is an excellent predictor of the interleukin-2 receptor-alpha status after treatment with daclizumab. *Transplantation* 77:281–286, 2004.
11. Hricik DE, Rodriguez V, Riley J, Bryan K, Tary-Lehmann M, Greenspan N, Dejelo C, et al.: Enzyme linked immunosorbent spot (ELISPOT) assay for interferon-gamma independently predicts renal function in kidney transplant recipients. *Am J Transplant* 3:878–884, 2003.
12. Olsen JV, Blagoev B, Gnad F, Macek B, Kumar C, Mortensen P, Mann M: Global, *in vivo*, and site-specific phosphorylation dynamics in signaling networks. *Cell* 127:635–648, 2006.
13. Belle A, Tanay A, Bitincka L, Shamir R, O'Shea EK: Quantification of protein half-lives in the budding yeast proteome. *Proc Natl Acad Sci U S A* 103: 13004–13009, 2006.
14. Yokoyama Y, Terai S, Ishikawa T, Aoyama K, Urata Y, Marumoto Y, Nishina H, et al.: Proteomic analysis of serum marker proteins in recipient mice with liver cirrhosis after bone marrow cell transplantation. *Proteomics* 6:2564–2570, 2006.
15. Lazzarotto-Silva C, Binato R, Rocher BD, Costa JA, Pizzatti L, Bouzas LF, Abdelhay E: Similar proteomic profiles of human mesenchymal stromal cells from different donors. *Cytotherapy* 11:268–277, 2009.
16. Wittke S, Haubitz M, Walden M, Rohde F, Schwarz A, Mengel M, Mischak H, et al: Detection of acute tubulointerstitial rejection by proteomic analysis of urinary samples in renal transplant recipients. *Am J Transplant* 5: 2479–2488, 2005.
17. Schaub S, Wilkins JA, Antonovici M, Krokhin O, Weiler T, Rush D, Nickerson P: Proteomic-based identification of cleaved urinary beta2-microglobulin as a potential marker for acute tubular injury in renal allografts. *Am J Transplant* 5:729–738, 2005.
18. Kienzl K, Sarg B, Golderer G, Obrist P, Werner ER, Werner-Felmayer G, Lindner H, et al.: Proteomic profiling of acute cardiac allograft rejection. *Transplantation* 88:553–560, 2009.
19. Nelsestuen GL, Martinez MB, Hertz MI, Savik K, Wendt CH: Proteomic identification of human neutrophil alpha-defensins in chronic lung allograft rejection. *Proteomics* 5:1705–1713, 2005.
20. Pan TL, Wang PW, Huang CC, Goto S, Chen CL: Expression, by functional proteomics, of spontaneous tolerance in rat orthotopic liver transplantation. *Immunology* 113:57–64, 2004.
21. Cheng J, Zhou L, Jiang JW, Qin YS, Xie HY, Feng XW, Gao F, et al.: Proteomic analysis of differentially expressed proteins in rat liver allografts developed acute rejection. *Eur Surg Res* 44:43–51, 2010.
22. Massoud O, Heimbach J, Viker K, Krishnan A, Poterucha J, Sanchez W, Watt K, et al.: Noninvasive diagnosis of acute cellular rejection in liver transplant recipients: a proteomic signature validated by enzyme-linked immunosorbent assay. *Liver Transpl* 17:723–732, 2011.
23. Kamada N, Calne RY: Orthotopic liver transplantation in the rat. Technique using cuff for portal vein anastomosis and biliary drainage. *Transplantation* 28:47–50, 1979.
24. Banff schema for grading liver allograft rejection: an international consensus document. *Hepatology* 25:658–663, 1997.
25. Alban A, David SO, Bjorkesten L, Andersson C, Sloge E, Lewis S, Currie I: A novel experimental design for comparative two-dimensional gel analysis: two-dimensional difference gel electrophoresis incorporating a pooled internal standard. *Proteomics* 3:36–44, 2003.
26. Zhang C, Wei J, Zheng Z, Ying N, Sheng D, Hua Y: Proteomic analysis of *Deinococcus radiodurans* recovering from gamma-irradiation. *Proteomics* 5: 138–143, 2005.
27. Xu M, Alwahsh SM, Ramadori G, Kollmar O, Slotta JE: Upregulation of hepatic melanocortin 4 receptor during rat liver regeneration. *J Surg Res* [epub ahead of print] 25 Dec 2013.
28. Immenschuh S, Song DX, Satoh H, Muller-Eberhard U: The type II hemopexin interleukin-6 response element predominates the transcriptional regulation of the hemopexin acute phase responsiveness. *Biochem Biophys Res Commun* 207:202–208, 1995.
29. Ahmad S, Sultan S, Naz N, Ahmad G, Alwahsh SM, Cameron S, Moriconi F, et al.: Regulation of Iron Uptake in Primary Culture Rat Hepatocytes: The Role of Acute Phase Cytokines. *Shock* 41:337–345, 2014.
30. Alwahsh SM, Xu M, Seyhan HA, Ahmad S, Mihm S, Ramadori G, Schultze FC: Diet high in fructose leads to an overexpression of lipocalin-2 in rat fatty liver. *World J Gastroenterol* 20(7):1807–1821, 2014.
31. Hvidberg V, Maniecki MB, Jacobsen C, Hojrup P, Moller HJ, Moestrup SK: Identification of the receptor scavenging hemopexin-heme complexes. *Blood* 106:2572–2579, 2005.

32. Brass CA, Immenschuh S, Song DX, Liem HH, Eberhard UM: Hemopexin decreases spontaneous chemiluminescence of cold preserved liver after reperfusion. *Biochem Biophys Res Commun* 248:574–577, 1998.
33. Baird SK, Kurz T, Brunk UT: Metallothionein protects against oxidative stress-induced lysosomal destabilization. *Biochem J* 394:275–283, 2006.
34. Geuken E, Buis CI, Visser DS, Blokzijl H, Moshage H, Nemes B, Leuvenink HG, et al.: Expression of heme oxygenase-1 in human livers before transplantation correlates with graft injury and function after transplantation. *Am J Transplant* 5:1875–1885, 2005.
35. Spiller F, Costa C, Souto FO, Vinchi F, Mestriner FL, Laure HJ, Alves-Filho JC, et al.: Inhibition of neutrophil migration by hemopexin leads to increased mortality due to sepsis in mice. *Am J Respir Crit Care Med* 183:922–931, 2011.
36. Smith A, Eskew JD, Borza CM, Pendrak M, Hunt RC: Role of heme-hemopexin in human T-lymphocyte proliferation. *Exp Cell Res* 232:246–254, 1997.
37. Naz N, Moriconi F, Ahmad S, Amanzada A, Khan S, Mihm S, Ramadori G, et al.: Ferritin L is the sole serum ferritin constituent and a positive hepatic acute-phase protein. *Shock* 39:520–526, 2013.
38. Rish KR, Swartzlander R, Sadikot TN, Berridge MV, Smith A: Interaction of heme and heme-hemopexin with an extracellular oxidant system used to measure cell growth-associated plasma membrane electron transport. *Biochim Biophys Acta* 1767:1107–1117, 2007.
39. Fagoonee S, Caorsi C, Giovarelli M, Stoltenberg M, Silengo L, Altruda F, Camussi G, et al.: Lack of plasma protein hemopexin dampens mercury-induced autoimmune response in mice. *J Immunol* 181:1937–1947, 2008.